

PMSM Sensorless Speed Control Drive

Youakim Kalaani¹, Rami Haddad², Adel El Shahat³

¹Department of Electrical Engineering, Georgia Southern University, USA

²Department of Electrical Engineering, Georgia Southern University, USA

³Department of Electrical Engineering, Georgia Southern University, USA

Abstract— Permanent magnet synchronous machines (PMSM) are very popular in many industrial applications such as in mechatronics, automotive, energy storage flywheels, centrifugal compressors, vacuum pumps, and robotics. This paper proposes Sensorless control for a PMSM speed drive which is based on a closed loop control system using a proportional and integral (PI) controller that is designed to operate in flux weakening regions under a constant torque angle. This sensorless element was adopted for best estimating the PMSM rotor position based on its performance characteristics eliminating the need for speed sensors which are usually required in such control applications. To achieve this goal, a pulse width modulation (PWM) control scheme was developed to work in conjunction with a field oriented motor control drive using Simulink. This innovative control system was simulated assuming realistic circuit components to maximize the accuracy of the proposed model. Finally, simulation results obtained under different operation conditions at below and above the rated speed of the motor were presented and discussed in this paper.

Index Terms—Permanent Magnet, Synchronous machine, Control, Sensorless, Simulink and Field Oriented.

I INTRODUCTION

The vector control of ac machines was introduced in the late 1960s by Blaschke, Hasse, and Leonhard in Germany. Following their pioneering work, this technique, allowing for the quick torque response of ac machines similar to that of dc machines, has achieved a high degree of maturity and become popular in a broad variety of applications. For many years, PMSM have been the subject of intense studies and various speed control schemes have been proposed in the literature. For instance, C. Bowen et al. [1] have addressed the modeling and simulation of PMSM supplied from a six step continuous inverter based on state space method. Furthermore, C. Mademlis et al. [2] presented an efficiency optimization method for vector-controlled interior drive, and a modular control approach was applied by X. Jian-Xin et al [3]. In motor drive applications, a shaft encoder or a hall sensor is typically used to measure the rotor position [4-8]. Due to the flux-weakening technology, the operating speed range can be extended by applying negative magnetizing current component to weaken the air-gap flux [9, 10]. This has led to a new design concept of permanent magnet (PM) machine for flux-weakening operation proposed by L. Xu et al. [11]. For their part, Tapia et al. have explored a magnetic structure termed the consequent-pole (CPPM) machine which had inherent field weakening capability [12]. Soong and Miller proved that maximum torque field-weakening control can be achieved through optimal high-saliency interior PM motor design [13] and a two control techniques to enhance the performance of PM drives over an extended speed range were

presented by Macminn and Jahns [14]. However, the techniques of maximum torque per ampere (MTPA) operation at a break-point speed was first investigated by Sebastian and Slemon [15] and a current-regulated flux-weakening method for reduced air-gap flux was introduced by Dhaoudi and Mohan [16]. Although current vector control and feed-forward decoupling compensation appeared in work done by Morimoto et al [17,18], it was not until Sudhoff et al [19] who set forth a flux-weakening control scheme that is relatively simple and does not require prior knowledge of the machine and inverter parameters. Along these lines, Sozer and Torrey [20] presented an adaptive control over the entire speed range of PM motor. Several flux-weakening control methods based on voltage regulation were proposed by Y. S. Kim et al [21], J. M., Kim et al [22], and J. H. Song et al [23] in which the voltage error signal is generated between the maximum output voltage and the voltage command. In vector control of PM motors, the output of the voltage regulator is used to determine the required demagnetizing current needed to prevent saturation. However, the added controller could only operate properly under well-tuned conditions which are not easily reached [24] and the d-q axis currents cannot be independently controlled due to the cross-coupling effects which become dominant at high speeds. As a result, the dynamic performance of PM motors are degraded without the presence of a decoupling control scheme and effective control of fast dynamic response requires accurate rotor position [21-27]. Adaptive control methods seem to

be the most promising modern control strategy [28], [29] and a model reference adaptive control (MRAC) scheme characterized by reduced computation was proposed by Cerruto et al [28]. This model was further refined by Baik et al [30] by estimating the values of slowly varying parameters using Lyapunov stability criteria. The use of sensors to measure motor speed can result in increased cost and reduced control robustness and/or reliability. The first breakthrough in sensorless control theory was reported by A. Rostami, and B. Asaei [31] who developed a method for estimating the rotor position as well as other proposed methods [32-35]. However, many challenges remain in the design of sensorless control to operate over a wide speed range of PM motors. Improved position-sensorless control schemes were developed in the last decade [36-40], especially in the concept area of direct drive which achieved higher dynamic response, increased efficiency, and low acoustic noise. In modern applications, the PMSM machine is designed to operate in constant torque and power modes at below and above the rated speed which can significantly reduce the cost and size of the overall drive system. The constant-torque operation can easily be achieved by conventional vector control but the motor will not be able to operate in constant-torque mode at above the rated speed. However, this problem was alleviated by the introduction of flux-weakening techniques which extended the operating speed range by applying negative magnetizing current component to weaken the air-gap flux [41], [42].

In this paper, a sensorless vector control of PMSM drive using flux weakening techniques is presented. A PI controller operating under constant-torque angle is implemented using a novel PWM control scheme for field oriented motor control drive. This controller was tested using Simulink and different operation conditions under variable speed were presented and discussed in this paper. This sensorless drive system is also useful in Electric Vehicle (EV) applications.

II PMSM DYNAMIC MODELING

The PMSM drive system with and without speed sensor is described in this section. It includes different components such as permanent magnet motors, position sensors, inverter, and current controller with sensor and speed estimation unit for sensorless control. Both components are presented in Fig.1 and Fig.2 respectively.

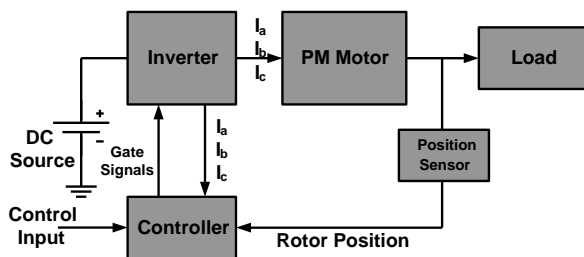


Fig.1-Drive System Schematic with position sensor

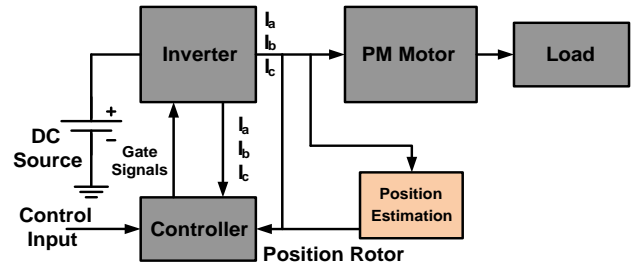


Fig.2-Drive System Schematic without position sensor

The PMSM equivalent circuit used to derive the dynamic equations in the d-q axis is presented in Fig.3.

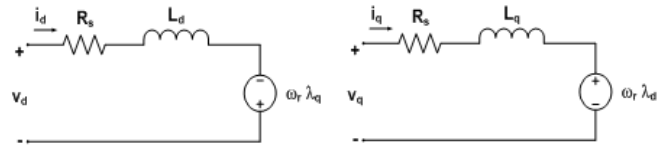


Fig.3- PMSM Equivalent Circuit

The stator windings are assumed to have equal turns per phase in the d-q axis. The rotor flux is also assumed to be concentrated along the d-axis while there is zero flux along the q-axis. In addition, it is assumed that the machine core losses are negligible. Variations in rotor temperature can alter the magnet flux but its variation with respect to time is considered to be negligible.

III PMSM STATOR FLUX – LINKAGE

The equations for the stator flux-linkage along the d-q axis are given by:

$$v_q = R_q i_q + \rho(\lambda_q) + \omega_r \lambda_d \quad (1)$$

$$v_d = R_d i_d + \rho(\lambda_d) - \omega_r \lambda_q \quad (2)$$

Where: ρ : is the d/dt differential factor; R_q, R_d are the winding resistances and referred as R_s when equal.

The q-d axis stator flux linkages reflected to the rotor reference frames can be written as:

$$\lambda_q = L_s i_q + L_{af} i_f \quad (3)$$

$$\lambda_d = L_s i_d + L_{af} i_f \quad (4)$$

Theoretically, the self-inductances of the stator q-d axis are equal to L_s only when the rotor magnets are at 180° electrical degrees apart but this is hardly the case in practice. When the stator winding is aligned with the rotor, the inductance L_d (d-axis) is the lowest while the winding facing the interpolar path results in higher inductance L_q (q-axis) [43]. The excitation of the permanent magnet is modeled as a constant current source i_f along the d-axis. Since there is no flux along the q-axis, the rotor current is assumed to be zero. Therefore, the flux linkages can be written as:

$$\begin{aligned}
 v_q &= R_s i_q + \rho (\lambda_q) + \omega_r \lambda_d \\
 v_d &= R_s i_d + \rho (\lambda_d) - \omega_r \lambda_q \\
 \lambda_q &= L_q i_q \\
 \lambda_d &= L_d i_d + L_m i_{fr} = L_d i_d + \lambda_{af} \\
 \lambda_{af} &= L_m i_{fr}
 \end{aligned}$$

Where: L_m is the mutual inductance between stator and rotor windings; ω_r : Electrical velocity of the rotor; λ_{af} : Flux linkage due to rotor; $\rho (\lambda_{af}) = 0$, $\lambda_{af} = L_m i_{fr}$; ρ : Operator.

IV PMSM TORQUE EQUATIONS

The electromagnetic torque is given by:

$$T_e = \frac{3P}{2} (\lambda_d i_q - \lambda_q i_d) \quad (5)$$

This torque is derived from the input power as follow:

$$P_{in} = v_a i_a + v_b i_b + v_c i_c \quad (6)$$

Equation (6) has three parts; 1) power loss in the conductors; 2) energy rate of change in the magnetic field; and 3) conversion to mechanical energy.

The electromechanical power is given by

$$P_{em} = \omega_{rm} T_e = (3/2) \omega_r (\lambda_d i_q - \lambda_q i_d) \quad (7)$$

$$\omega_r = (P/2) \omega_{rm} \quad (8)$$

Where: P is the number of poles and ω_{rm} the mechanical velocity of the rotor.

Therefore, the torque can be written as

$$T_e = \frac{3P}{2} (\lambda_{af} i_q + (L_d - L_q) i_d i_q) \quad (9)$$

Where, the first term of equation (9) presents the magnet alignment and the second term presents the torque reluctance.

The general mechanical equation for the motor is written as

$$T_e = T_l + T_d + B \omega_{rm} + J \rho \omega_{rm} \quad (10)$$

Where: B : Viscous frictions coefficient; J : Inertia of the shaft and load system; T_d : Dry friction; T_l : Load torque

V PMSM DYNAMIC SIMULATION

The dynamic simulation presented in this paper was performed using Simulink in MATLAB package. A PMSM block is shown in Fig. 4 where the voltage and load torque are presented as inputs while the motor speed and current are presented as outputs.

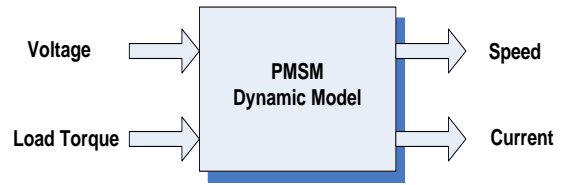


Fig.4- Model Block of PMSM Dynamic

A more detailed model [44-46] is provided in Fig. 5.

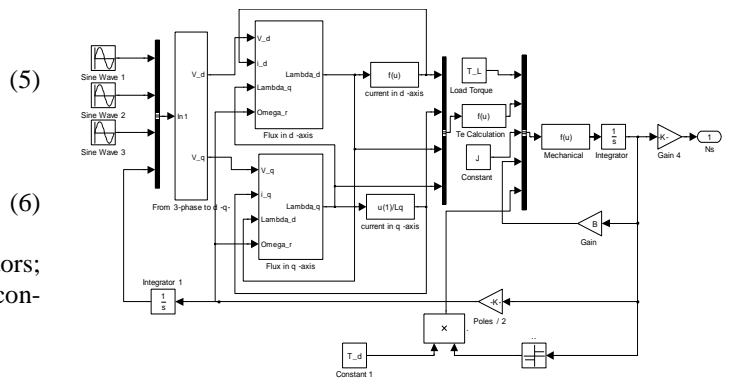


Fig.5- Detailed Model of PMSM

VI PMSM CURRENT CONTROL

High-performance drives utilize control strategies which develop command signals for the AC machine currents. Current control eliminates stator dynamics (effects of stator resistance, stator inductance, and induced EMF) and thus, to the extent that the current regulator functions as an ideal current supply, the order of the system can significantly be reduced. However, AC current regulators which form the inner loop of the drive system are complex since both amplitude and phase shift of the stator currents must be controlled. They must provide minimum steady-state error and also require the widest bandwidth in the system. Both current source inverters (CSI) and voltage source inverters (VSI) can be operated in controlled current modes. PWM current controllers [47] are widely used since they can generate a control scheme based on comparing a triangular carrier wave of desired switching frequency to the error of the controlled signal. The error is the difference between the reference signal generated in the controller and the actual motor current. If the error command is above the triangle waveform, the VSI leg is held switched to the positive polarity (upper switch on). Contrarily, if the error command is below the triangle waveform, the inverter leg is switched to the negative polarity (lower switch on). In this study, a PWM current controller is used with generated signals as shown in Fig. 6.

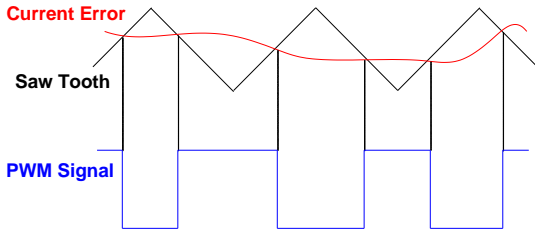


Fig.6- PWM Current Controller

VII PMSM FIELD ORIENTED CONTROL

A PMSM field oriented or vector control is derived from the machine dynamic model and it is based on the decoupling of the torque components. The 3-phase currents flown in the stator windings can be transformed to the rotor reference frame using Park's transformation as follow:

$$\begin{aligned} i_a &= I_s \sin(\omega_r t + \alpha) \\ i_b &= I_s \sin(\omega_r t + \alpha - \frac{2\pi}{3}) \\ i_c &= I_s \sin(\omega_r t + \alpha + \frac{2\pi}{3}) \end{aligned} \quad (11)$$

Where α is the angle between the rotor field and stator current; ω_r is the electrical rotor speed.

In the rotor reference frame, the q- axis current (i_q) and the d- axis current (i_d) are usually constant since α is fixed for a given load torque. Under this condition, i_q and i_d are called respectively the torque and flux producing components of the stator current. They can be written as:

$$\begin{pmatrix} i_q \\ i_d \end{pmatrix} = I_s \begin{pmatrix} \sin \alpha \\ \cos \alpha \end{pmatrix} \quad (12)$$

And, the electromagnetic torque is given by:

$$T_e = \frac{3}{2} \frac{P}{2} \left[\frac{1}{2} (L_d - L_q) I_s^2 \sin 2\alpha + \lambda_{af} I_s \sin \alpha \right] \quad (13)$$

The field oriented or vector control can be utilized under two modes of operation:

A Constant Flux Operation

In this mode of operation, it is possible to produce maximum torque by setting angle α in equation (12) to 90° which makes i_d zero and i_q equals to I_s . Therefore, torque equation (13) can be rewritten as a function of the motor current:

$$T_e = k_t \cdot I_q \quad (14)$$

$$k_t = \left(\frac{3}{2}\right) \left(\frac{P}{2}\right) \lambda_{af} \quad (15)$$

B Flux-weakening Operation

Flux weakening is the process of reducing the flux in the d-axis which yields higher speed range. The weakening of the field flux is required for operation above the rated speed or base frequency. Under this mode, the motor drive is operated at a constant voltage over frequency (V/F) ratio which results in a reduction of the torque proportional to the change in the frequency. Under this condition, the motor operates in the constant power region [48]. When permanent magnets are used, flux-weakening is achieved by increasing the negative i_d current and using armature reaction to reduce the air-gap flux [49]. The torque can be varied by altering the angle between the stator MMF and the rotor d-axis. In the flux weakening region where $\omega_r > \omega_{rated}$, it is possible to change the value of α by adjusting i_d and i_q as shown below

$$\alpha = \tan^{-1} \left(\frac{i_q}{i_d} \right) \quad (16)$$

Since torque is a function of i_q current, the torque will also be reduced. The generated reference signals are used by the current controller to drive the inverter and the load torque given by equation (17) can be adjusted for different reference speeds ω_r

$$T_l = T_{e(rated)} \left(\frac{\omega_{rated}}{\omega_r} \right) \quad (17)$$

VIII IMPLEMENTING SPEED CONTROL LOOP

The precise control of speed and position is required in many applications such as in robotics and factory automation. A typical control system consists of a speed feedback system, a motor, an inverter, a controller, and a speed setting device. A properly designed feedback controller makes the system insensitive to disturbance and changes of the parameters. Closed-Loop control systems have fast response but are expensive due to the need of feedback components such as speed sensors. A block diagram of a typical PMSM drive system with a full speed range is shown in Fig. 7. The system consists of a motor, an inverter, a controller (constant flux and flux-weakening operation, and reference signals)

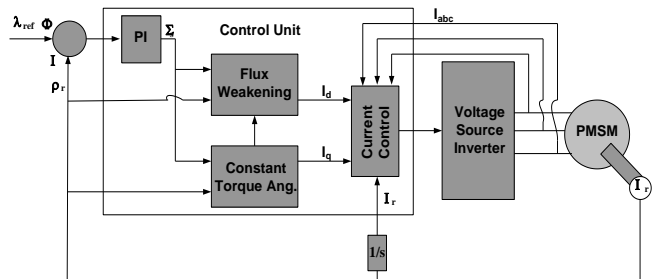


Fig.7- Block Diagram for original drive system

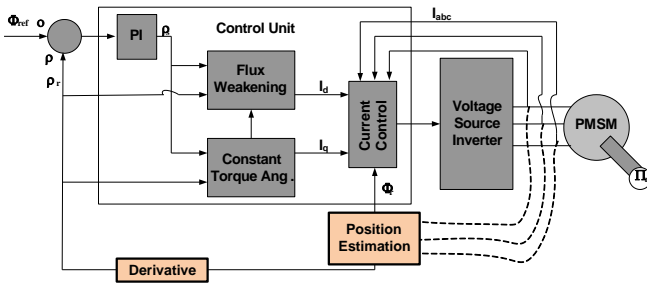


Fig.8- Block Diagram for Sensorless drive system

A PMSM speed Sensorless drive system is shown in Fig. 8 in which the speed sensor is replaced by a position estimation and its derivative.

Speed controller calculates the difference between the reference speed and the actual speed producing an error which is fed to the PI controller. PI controllers are widely used for motion control systems. They consist of a proportional gain that produces an output proportional to the input error and an integration to eliminate the steady state error due to a step input. A block diagram for a typical PI controller is shown in Fig. 9.

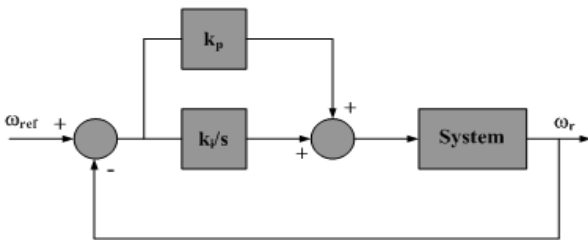


Fig. 9- Block Diagram of a PI Controller

Motor speed controllers consist of an inner loop for the current and an outer loop for the speed. Depending on the response of the system, the current loop is at least 10 times faster than the speed loop. The current control is performed by the comparison of the reference currents with the actual motor currents. A simplified control system may be obtained by setting the gain of the current loop to unity as displayed in Fig. 10.

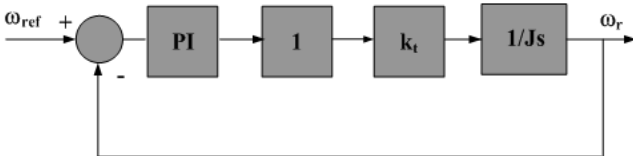


Fig.10- Simplified Speed Controller Block Diagram

The equivalent circuit of an inverter used for PMSM speed drive is provided in Fig. 11.

$$\begin{aligned} v_{ab}(t) &= v_{an}(t) - v_{bn}(t) \\ v_{bc}(t) &= v_{bn}(t) - v_{cn}(t) \\ v_{ca}(t) &= v_{cn}(t) - v_{an}(t) \end{aligned} \quad (18)$$

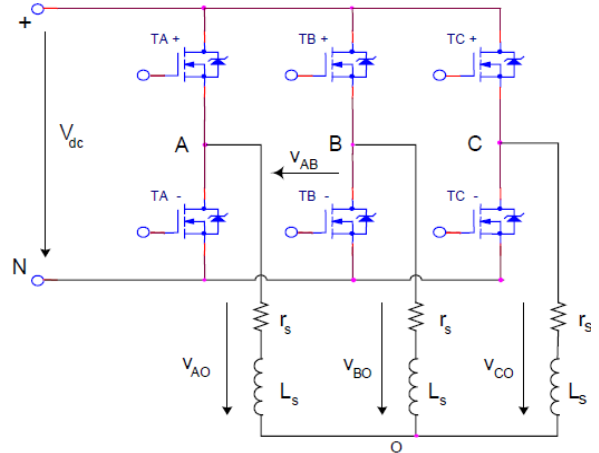


Fig. 11- Inverter-motor equivalent circuit

The motor voltages provided by the inverter are equivalent to a 3-phase voltage source [50,51] that can be written with a modified expression as:

$$\begin{aligned} v_{ao}(t) &= v_{an}(t) - v_{on}(t) \\ v_{bo}(t) &= v_{bn}(t) - v_{on}(t) \\ v_{co}(t) &= v_{cn}(t) - v_{on}(t) \end{aligned} \quad (19)$$

For a star connected system, the following relationship must be satisfied at all time:

$$v_{ao} + v_{bo} + v_{co} = 0 \quad (20)$$

Using equations (19) and (20), the null voltage is derived as:

$$v_{on} = (v_{an} + v_{bn} + v_{cn})/3 \quad (21)$$

The phase voltages collected at the inverter leg are a function of the dc source and the switching time (da,db,dc) as follows:

$$\begin{aligned} v_{an} &= V_{dc} \cdot da \\ v_{bn} &= V_{dc} \cdot db \\ v_{cn} &= V_{dc} \cdot dc \end{aligned} \quad (22)$$

From which the line voltages can be derived as:

$$\begin{aligned} v_{ab} &= V_{dc} \cdot (da - db) \\ v_{bc} &= V_{dc} \cdot (db - dc) \\ v_{ca} &= V_{dc} \cdot (dc - da) \end{aligned} \quad (23)$$

With further derivation, the phase voltages can be written as:

VIII INVERTER-MOTOR EQUIVALENT CIRCUIT

$$\begin{aligned} v_a &= V_{dc} \cdot (da - (da + db + dc) / 3) \\ v_b &= V_{dc} \cdot (db - (da + db + dc) / 3) \\ v_c &= V_{dc} \cdot (dc - (da + db + dc) / 3) \end{aligned} \quad (24)$$

The dc-link voltage V_{dc} , may be obtained using V_{sn} (maximum phase voltage) as follow [52]:

$$V_{dc} = \frac{2 \cdot P}{\pi} \cdot \sin\left(\frac{\pi}{P}\right) \cdot V_{sn} \quad (25)$$

Where V_{sn} : peak amplitude of phase voltage

IX OBSERVER FOR SPEED ESTIMATION

A position-sensorless PMSM drive makes use of an observer instead of a sensor or encoder to estimate the speed of the motor. This concept is based on the two-axis theory to derive an equivalent quadrature-phase model to represent the three-phase machine. In fact, the d-axis and q-axis currents are related to the actual three-phase stator currents by the following transformation:

$$\vec{i}_{\alpha\beta 0s} = T_{abc \rightarrow \alpha\beta 0} \cdot \vec{i}_{abc} \quad (26)$$

Where

$$T_{\alpha\beta 0} = \frac{2}{3} \begin{bmatrix} 1 & -\frac{1}{2} & -\frac{1}{2} \\ 0 & \frac{\sqrt{3}}{2} & -\frac{\sqrt{3}}{2} \\ \frac{1}{2} & \frac{1}{2} & \frac{1}{2} \end{bmatrix} \quad (27)$$

Conversion to the new stationary (α - β) frame is also known as Clark Transformation (insert referenc here). Similarly, voltage (V) and flux linkage (λ) can also be transferred from (a - b - c) frame to (α - β) frame by the following transformations:

$$\vec{v}_{\alpha\beta 0s} = r_{\alpha\beta 0s} \cdot \vec{i}_{\alpha\beta 0s} + p \cdot \vec{\lambda}_{\alpha\beta 0s} \quad (28)$$

where

$$\begin{aligned} \vec{v}_{\alpha\beta 0s} &= \begin{bmatrix} v_{\alpha s} & v_{\beta s} & v_{0s} \end{bmatrix}^T \\ \vec{i}_{\alpha\beta 0s} &= \begin{bmatrix} i_{\alpha s} & i_{\beta s} & i_{0s} \end{bmatrix}^T \\ \vec{\lambda}_{\alpha\beta 0s} &= \begin{bmatrix} \lambda_{\alpha s} & \lambda_{\beta s} & \lambda_{0s} \end{bmatrix}^T \end{aligned} \quad (29)$$

The flux linkage is transformed as

$$\vec{\lambda}_{\alpha\beta 0s} = L_{\alpha\beta 0s} \cdot \vec{i}_{\alpha\beta 0s} + \vec{\lambda}_{\alpha\beta 0m} \quad (30)$$

where

$$\vec{\lambda}_{\alpha\beta 0m} = \lambda_{\alpha\beta 0m} \begin{bmatrix} \cos \theta_r \\ \sin \theta_r \\ 0 \end{bmatrix} \quad (31)$$

Furthermore, the induced back EMF in the windings of the fictitious quadrature-phase machine can be written as a function of the flux linkages and rotor position (angle) as:

$$\vec{e}_{\alpha\beta s} = \begin{bmatrix} e_{\alpha s} \\ e_{\beta s} \end{bmatrix} = \omega_r \lambda_m \begin{bmatrix} -\sin \theta_r \\ \cos \theta_r \end{bmatrix} \quad (32)$$

Finally, the stator I_{abc} currents can readily be obtained from the I_{dq0} currents by the following reverse transformation:

$$\begin{bmatrix} I_a \\ I_b \\ I_c \end{bmatrix} = \begin{bmatrix} \cos \theta & \sin \theta & 1 \\ \cos(\theta - 120) & \sin(\theta - 120) & 1 \\ \cos(\theta + 120) & \sin(\theta + 120) & 1 \end{bmatrix} \begin{bmatrix} I_q \\ I_d \\ I_0 \end{bmatrix} \quad (33)$$

X SIMULINK SIMULATION OF PMSM DRIVE

Simulink was chosen from several simulation tools because of its flexibility in working with analog and digital devices. The PMSM drive system presented in this paper was made of several block diagrams as shown in the following figures using Simulink and then connected together to build the whole system. For instance, I_{dq0} to I_{abc} reverse transformation block is shown in Fig 12, the vector control reference current block with PI speed controller depicted in Fig.13, the voltage source inverter shown in Fig. 14, and the sensorless rotor position estimation block is given in Fig 16. The block diagram for the complete PMSM drive system is presented in Fig. 17. For simulation purposes, the voltages are assumed to be the system inputs and the current are the outputs. Clark Transformation blocks with the flux linkages block were simulated to estimate the rotor position and Parks transformation were used for converting V_{abc} to V_{dq0} . Also as shown, vector control requires a block for the calculation of the reference current using angle α , rotor position, and the magnitude of current I_s . Inverter action is implemented using reference currents to generate the gate pulses for the IGBTs.

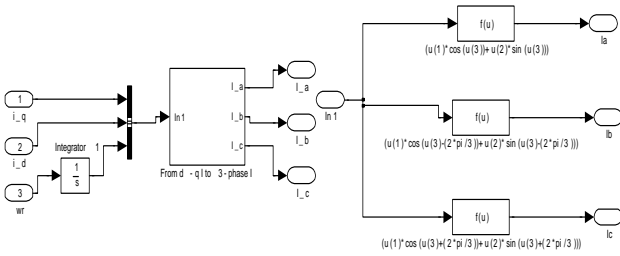


Fig. 12- I_{dq0} to I_{abc} Block

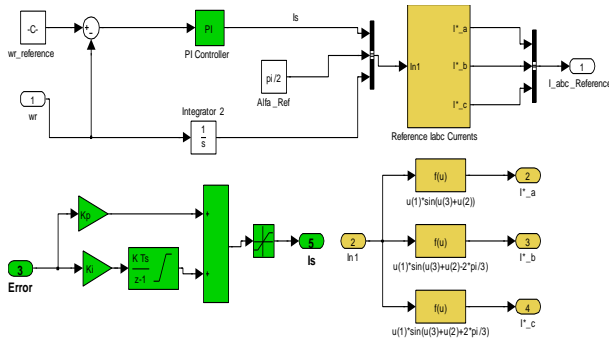


Fig. 13- Vector Control Reference Current Block with PI Speed Controller

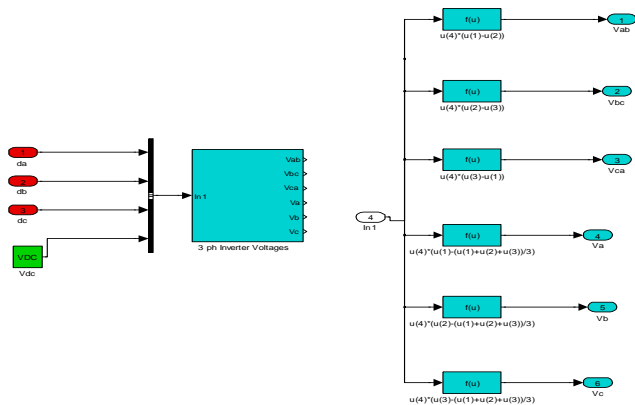


Fig. 14- Voltage Source Inverter

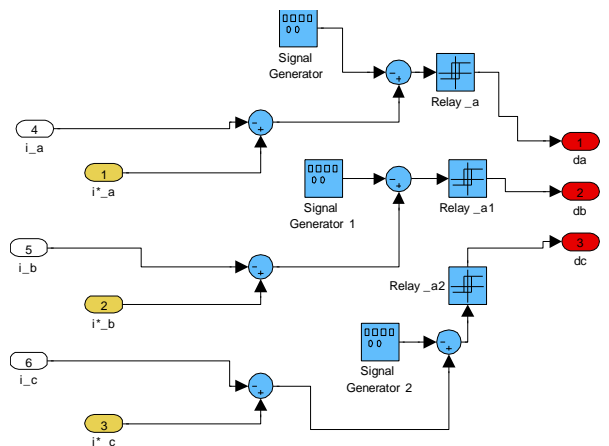


Fig. 15- PWM current controller block

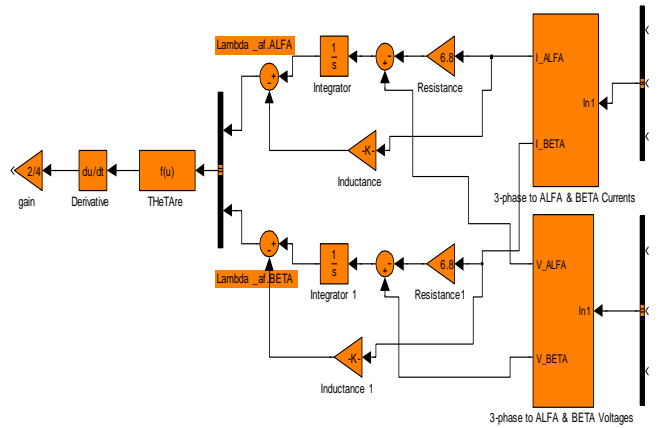


Fig. 16- Rotor Position (Speed Sensorless) Estimation block

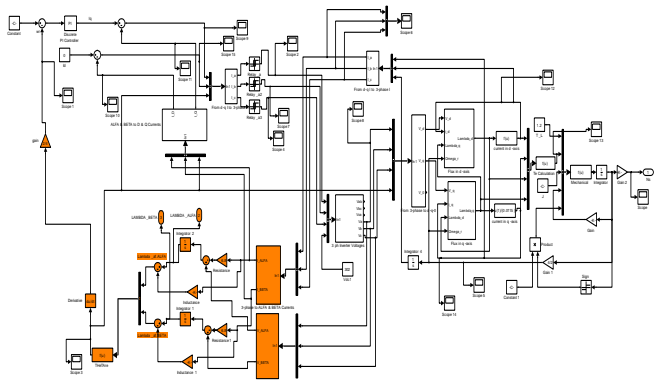


Fig. 17- Complete speed sensorless drive system

XI SIMULATION RESULTS

Simulation results of the PMSM drive system using the proposed PWM current control scheme are presented in this section. The motor was run in constant-torque mode below its rated speed (**what is it?**) and in flux-weakening mode above rated speed. Currents, torques, and speeds were all plotted under these two operation modes. Simulation results are given at motor speeds of 2000 rpm and 2400 rpm respectively. As shown in Fig 18 and Fig 26, the motor speed reached the desired speed levels in less than .01s with all oscillation died out within .02s. The steady state error due to a step input (reference speed voltage) was shown to be zero.

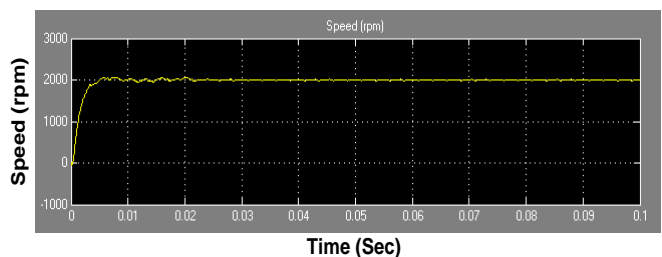


Fig.18- Motor Speed vs time at 2000 rpm

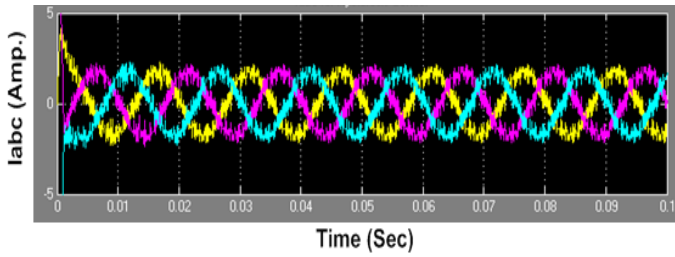


Fig.19 - I_{abc} Currents vstime at 2000 rpm

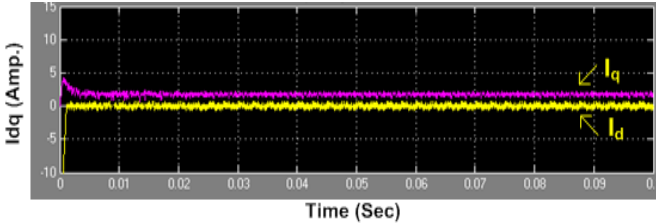


Fig. 20- I_{dq} Currents vstime at 2000 rpm

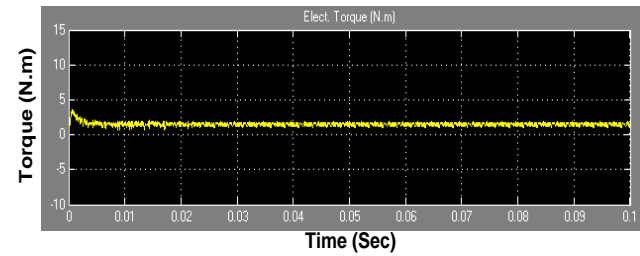


Fig.21- Torque vs time at 2000 rpm

The 3-phase I_{abc} currents drawn by the motor and obtained by Park's reverse transformation are shown for the two speeds in Fig 19 and 27 respectively. The corresponding I_{dq} currents are displayed in Fig. 20 and 28 in which the value of i_d in Fig 20 is zero since field oriented control is used. The torques developed by the motor were also shown in Fig. 21 and 29 where the starting torque is almost twice the steady state or rated torque value.

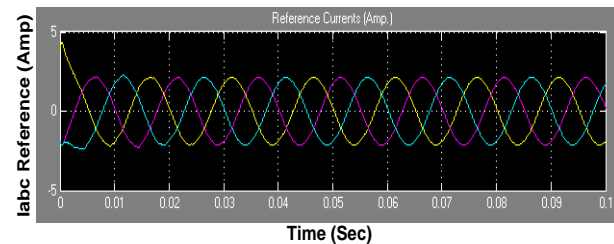


Fig 22- I_{abc} Reference Currents vstime at 2000 rpm

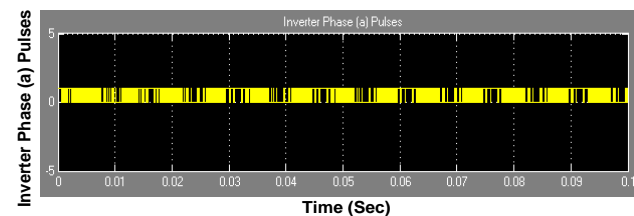


Fig23- Inverter Phase (a) Pulses vs time at 2000 rpm

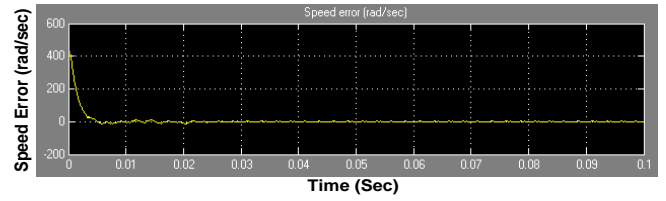


Fig 24- Speed Error vs time at 2000 rpm

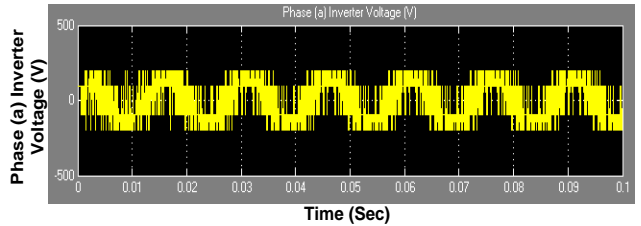


Fig 25 - Phase (a) Voltage vs time at 2000 rpm

Reference currents obtained by this type of control are shown in Fig 22 and 30. Phase (a) inverter pulse, speed, error, and inverter phase (a) voltage for 2000 rpm speed are presented in Fig 23, 24 and 25 respectively. And those for 2400 rpm speed are displayed in Fig 30, 31, and 32.

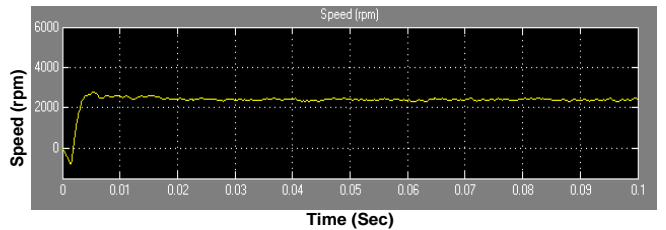


Fig 26- Motor Speed vs time at 2400 rpm

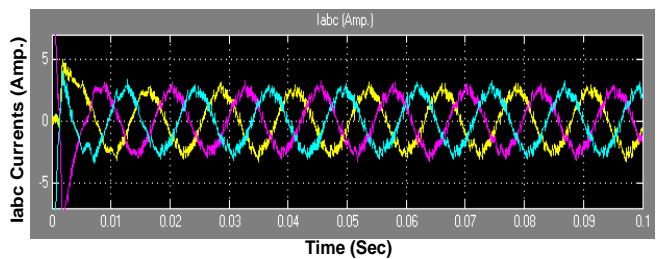


Fig 27- I_{abc} Currents vstime at 2400 rpm

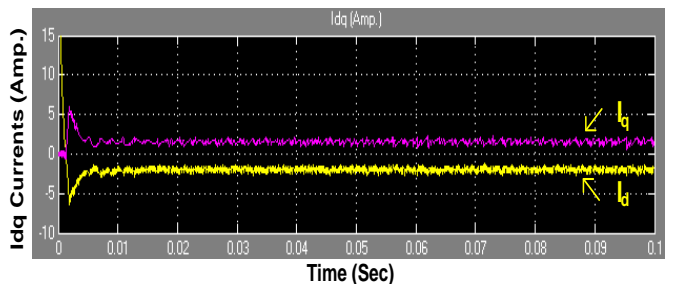


Fig 28- I_{dq} Currents vs time at 2400 rpm

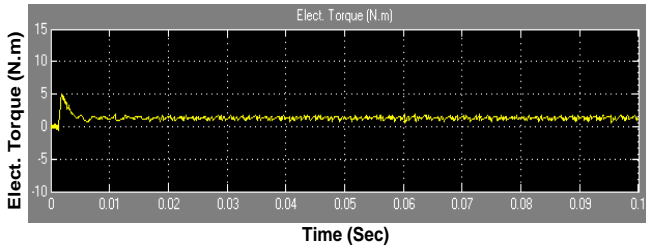


Fig. 29- Torque vs time at 2400 rpm

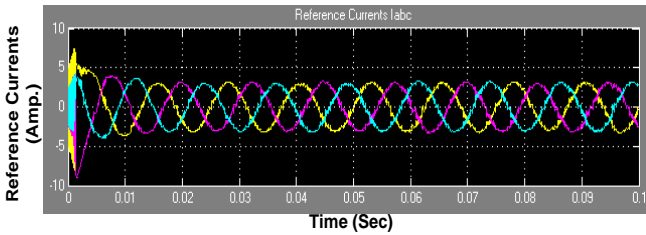


Fig 30- I_{abc} Reference Currents vs time at 2400 rpm

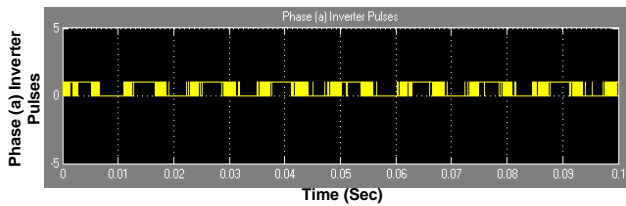


Fig 31-Inverter Phase (a) Pulses vs time at 2400 rpm

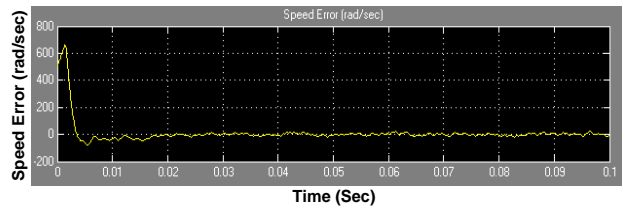


Fig 32-Speed Error with time at 2400 rpm

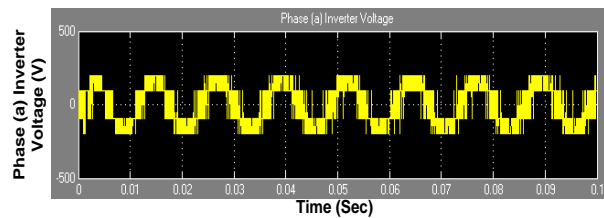


Fig 33- Phase (a) Voltage vs time at 2400 rpm

It should be noted that negative speed was observed in Fig 26 due to the speed acceleration effects which make the machine run as a generator at first before running as a motor. Without flux weakening, the torque was also observed to rapidly decrease to zero with increasing speed above the rated speed and briefly turned negative in response to sudden variations in the dc bus voltage. This mode of operation is unstable since the machine drive is out of control at that time. This can be resolved by flux weakening which can ensure proper control in the whole speed and volt-

age range. Furthermore, the negative effect of the pure feedback control could be avoided by torque setpoint rate limitation which is necessary to limit increase in acceleration anyway.

V CONCLUSION

Although a conclusion may review the main points of the paper, do not replicate the abstract as the conclusion. A conclusion might elaborate on the importance of the work or suggest applications and extensions. Authors are strongly encouraged not to call out multiple figures or tables in the conclusion—these should be referenced in the body of the paper.

REFERENCES

- [1] B. Cui, J. Zhou, and Z. Ren, "Modeling and simulation of permanent magnet synchronous motor drives," 2001.
- [2] C. Mademlis and N. Margaris, "Loss minimization in vector-controlled interior permanent-magnet synchronous motor drives," *Industrial Electronics, IEEE Transactions on*, vol. 49, pp. 1344-1347, 2002.
- [3] X. Jian-Xin, S. K. Panda, P. Ya-Jun, L. Tong Heng, and B. H. Lam, "A modular control scheme for PMSM speed control with pulsating torque minimization," *Industrial Electronics, IEEE Transactions on*, vol. 51, pp. 526-536, 2004.
- [4] R. Gabriel, W. Leonhard, and C. Nordby, "Field oriented control of standard AC motor using microprocessor," *IEEE Trans. Ind. Applicat.*, vol. IA-16, pp. 186-192, 1980.
- [5] L. Harnefors, "Design and analysis of general rotor-flux oriented vector control systems," *IEEE Trans. Ind. Electron.*, vol. 48, pp. 383-389, Apr. 2001.
- [6] M. Schroedl, "Sensorless control of AC machines at low speed and standstill based on the "INFORM" method," in *Conf. Rec. IEEE-IAS Annu. Meeting*, vol. 1, 1996, pp. 270-277.
- [7] P. L. Jansen and R. D. Lorenz, "Transducerless position and velocity estimation in induction and salient AC machines," *IEEE Trans. Ind. Applicat.*, vol. 31, pp. 240-247, Mar./Apr. 1995.
- [8] P. L. Jansen, R. D. Lorenz, and D. W. Novotny, "Observer-based direct field orientation: Analysis and comparison of alternative methods," *IEEE Trans. Ind. Applicat.*, vol. 30, pp. 945-953, July/Aug. 1994.
- [9] T. M. Jahns and V. Blasko, "Recent advances in power electronics technology for industrial and traction machine drives," *Proc. IEEE*, vol. 89, pp. 963-975, June 2001.
- [10] Thomas M. Jahns, "Motion control with permanent-magnet ac machines," in *Proc. IEEE*, vol. 82, Aug. 1994, pp. 1241-1252.
- [11] L. Xu, L. Ye, L. Zhen and A. El-Antably, "A new design

- concept of permanent magnet machine for flux weakening operation,” *IEEE Trans. Ind. Applicat.*, vol. 31, pp. 373-378, March/April, 1995.
- [12] J. A. Tapia, F. Leonardi, and T. A. Lipo, “Consequent-pole permanent-magnet machine with extended field-weakening capability,” *IEEE Trans. Ind. Applicat.*, vol. 39, pp. 1704-1709, Nov./Dec., 2003.
- [13] W. L. Soong and T. J. Miller, “Field-weakening performance of brushless synchronous AC motor drives,” *Proc. IEE—Elect. Power Applicat.*, vol. 141, no. 6, pp. 331–340, Nov. 1994.
- [14] S. R. Macminn and T. M. Jahns, “Control techniques for improved high-speed performance of interior PM synchronous motor drives,” *IEEE Trans. Ind. Applicat.*, vol. 2, pp. 997-1004, Sept./Oct. 1991.
- [15] T. Sebastian and G. R. Slemon, “Operating limits of inverter-driven permanent magnet motor drives,” *IEEE CH2272-3/86*, pp. 800-805, 1986.
- [16] R. Dhaouadi and N. Mohan, “Analysis of current-regulated voltage-source inverters for permanent magnet synchronous motor drives in normal and extended speed ranges,” *IEEE Trans. Energy Conv.*, vol. 5, pp. 137-144, Mar. 1990.
- [17] S. Morimoto, M. Sanada and K. Takeda, “Wide-speed operation of interior permanent magnet synchronous motors with high-performance current regulator,” *IEEE Trans. Ind. Applicat.*, vol. 30, pp. 920-926, July/Aug. 1994.
- [18] S. Morimoto, Y. Takeda, T. Hirasaka, and K. Taniguchi, “Expansion of operating limits for permanent magnet by current vector control considering inverter capacity,” *IEEE Trans. Ind. Applicat.*, vol. 26, pp. 866-871, Sept./Oct. 1990.
- [19] S. D. Sudhoff, K. A. Corzine and H. J. Hegner, “A flux-weakening strategy for current-regulated surface-mounted permanent-magnet machine drives,” *IEEE Trans. Energy Conv.*, vol. 10, pp. 431-437, Sept. 1995.
- [20] Y. Sozer and D. A. Torrey, “Adaptive Flux weakening control of permanent magnet synchronous motors,” in *Conf. Rec. IEEE-IAS Annu. Meeting*, vol. 1, St. Louis, MO, 1998, pp. 475–482.
- [21] Y. S. Kim, Y. K. Choi and J. H. Lee, “Speed-sensorless vector control for permanent-magnet synchronous motors based on instantaneous reactive power in the wide-speed region,” *IEE Proc-Electr. Power Appl.*, vol. 152, No. 5, pp. 1343-1349, Sept. 2005.
- [22] J. M. Kim and S. K. Sul, “Speed control of interior permanent magnet synchronous motor drive for the flux weakening operation,” *IEEE Trans. Ind. Applicat.*, vol. 33, pp. 43-48, Jan./Feb. 1997.
- [23] J. H. Song, J. M. Kim, and S. K. Sul, “A new robust SPMSM control to parameter variations in flux weakening region,” *IEEE IECON*, vol. 2, pp. 1193-1198, 1996.
- [24] J. J. Chen and K. P. Chin, “Automatic flux-weakening control of permanent magnet synchronous motors using a reduced-order controller,” *IEEE Trans. Power Electron.*, vol. 15, pp. 881-890, Sept. 2000.
- [25] A. Consoli, G. Scarcella and A. Testa, “Industry application of zero-speed sensorless control techniques for PM synchronous motors,” *IEEE Trans. Ind. Applicat.*, vol. 37, pp. 513-521, March/April, 2001.
- [26] M. Tursini, R. Petrella and F. Parasiliti, “Initial rotor position estimation method for PM motors,” *IEEE Trans. Ind. Applicat.*, vol. 39, pp. 1630-1640, Nov./Dec., 2003.
- [27] F. J. Lin and S. L. Chiu, “Adaptive fuzzy sliding mode control for PM synchronous servo motor drives,” *Proc. IEE—Contr. Theory Applicat.*, vol. 145, no. 1, pp. 63–72, 1998.
- [28] E. Cerruto, A. Consoli, A. Raciti, and A. Testa, “A robust adaptive controller for PM motor drives in robotic applications,” *IEEE Trans. Power Electron.*, vol. 10, pp. 62-71, Jan. 1995.
- [29] K. J. Åström and B. Wittenmark, “A survey of adaptive control applications,” in *Proc. 34th IEEE Conf. Decision and Control New Orleans, LA*, 1995, pp. 649-654.
- [30] I. C. Baik, K. H. Kim, and M. J. Youn, “Robust nonlinear speed control of PM synchronous motor using adaptive and sliding mode control techniques,” *Proc. IEE—Elect. Power Applicat.*, vol. 145, no. 4, pp. 369–376, 1998.
- [31] Alireza Rostami and Behzad Asaei, “A novel method for estimating the initial rotor position of PM motors without the position sensor,” *Energy Conversion and Management*, Vol. 50, (2009), pp. 1879–1883.
- [32] M.S. Merzoug and H. Benalla, “Nonlinear Backstepping Control of Permanent Magnet Synchronous Motor (PMSM),” *International Journal of Systems Control* (Vol.1-2010/Iss.1,),pp. 30-34.
- [33] Jinpeng Yu, Junwei Gao, Yumei Ma, and Haisheng Yu, “Adaptive Fuzzy Tracking Control for a Permanent Magnet Synchronous Motor via Backstepping Approach,” *Mathematical Problems in Engineering*, Hindawi Publishing Corporation, Volume 2010, Article ID 391846.
- [34] H.M. Hasanién, “Torque ripple minimization of permanent magnet synchronous motor using digital observer controller,” *Energy Conversion and Management*, Volume 51, issue 1 (January, 2010), pp. 98-104
- [35] Li Dong, Wang Shi-Long, Zhang Xiao-Hong and Yang Dan, “Impulsive control for permanent magnet synchronous motors with uncertainties: LMI approach,” *Chinese Physics B*, Vol.19, Issue1, pp.010506-7(2010). T. Markvart and L. Castaner, *Practical Handbook of Photovoltaics, Fundamentals and Applications*. Elsevier, 2003.
- [36] R. Gabriel, W. Leonhard, and C. Nordby, “Field oriented control of standard AC motor using microprocessor,” *IEEE Trans. Ind. Applicat.*, vol. IA-16, pp. 186–192, 1980.

- [37] L. Harnefors, "Design and analysis of general rotor-flux oriented vector controlsystems," IEEE Trans. Ind. Electron., vol. 48, pp. 383–389, Apr. 2001.
- [38] M. Schroedl, "Sensorless control of AC machines at low speed and standstill based on the "INFORM" method," in Conf. Rec. IEEE-IAS Annu. Meeting, vol. 1, 1996, pp. 270–277.
- [39] P. L. Jansen and R. D. Lorentz, "Transducerless position and velocity estimation in induction and salient AC machines," IEEE Trans. Ind. Applicat., vol. 31, pp. 240–247, Mar./Apr. 1995.
- [40] P. L. Jansen, R. D. Lorenz, and D. W. Novotny, "Observer-based direct field orientation: Analysis and comparison of alternative methods," IEEE Trans. Ind. Applicat., vol. 30, pp. 945–953, July/Aug. 1994.
- [41] T. M. Jahns and V. Blasko, "Recent advances in power electronics technology for industrial and traction machine drives," Proc. IEEE, vol. 89, pp. 963–975, June 2001.
- [42] Thomas M. Jahns, "Motion control with permanent-magnet ac machines," in Proc. IEEE, vol. 82, Aug. 1994, pp. 1241-1252.
- [43] R. Krishnan, *Electric Motor Drives: Modeling, Analysis & Control*, Prentice Hall, 2006.
- [44] H. M. El Shewy, F. E. Abd Al Kader, M. El Kholy, and A. El Shahat, "Dynamic Modeling of Permanent Magnet Synchronous Motor Using MATLAB - Simulink" EE108, 6th International Conference on Electrical Engineering ICEENG 6, 27-29 May 2008, Military Technical College, Egypt .
- [45] Adel El Shahat, and Hamed El Shewy, "Permanent Magnet Synchronous Motor Dynamic Modeling" Paper ID: X305, 2nd International Conference on Computer and Electrical Engineering (ICCEE 2009); Dubai, UAE, December 28 - 30, 2009.
- [46] Adel El Shahat, Hamed El Shewy, "PM Synchronous Motor Dynamic Modeling with Genetic Algorithm Performance Improvement", *International Journal of Engineering*, ISSN 2141-2839 (Online); ISSN 2141-2820 (Print); *Science and Technology* Vol. 2, No. 2, 2010, pp. 93-106.
- [47] B. K. Bose, *Power Electronics and Variable Frequency Drives*, 1 ed: Wiley, John & Sons, 1996.
- [48] R. Krishnan, *Electric Motor Drives Modeling, Analysis, and Control*, Pearson Education, 2001.
- [49] X. Junfeng, W. Fengyan, F. Jianghua, and X. Jianping, "Flux-weakening control of permanent magnet synchronous motor with direct torque control consideration variation of parameters," *Industrial Electronics Society, IECON 2004. 30th Annual Conference of IEEE*, Vol. 2, pp. 1323- 1326, 2004
- [50] Kazmierkowski M.P., Tunia H.: *Automatic Control Of Converter-Fed Drives*, Elsevier Science & Technology (United Kingdom), 1994
- [51] Ned Mohan, Tore M. Undeland and William P. Robbins, *Power electronics, Converters, Applications and Design*, Third Edition, USA ISBN 0-471-22693-9, John Wiley & Sons, Inc.
- [52] A. Munoz-Garcia and D. W. Novotny, "Utilization of Third Harmonic-Induced-Voltages in PM Generators," *Industry Applications Conference*, 1996. Thirty-First IAS Annual Meeting, IAS apos;96., Vol. 1, 6-10 Oct 1996, Page(s):525 – 532.